



# Effect of thermal and vibrational combined ageing on QFN terminal pads solder reliability

F. Arabi, A. Gracia, J.-Y. Delétage, H. Frémont

## ► To cite this version:

F. Arabi, A. Gracia, J.-Y. Delétage, H. Frémont. Effect of thermal and vibrational combined ageing on QFN terminal pads solder reliability. *Microelectronics Reliability*, 2020, pp.113883. 10.1016/j.microrel.2020.113883 . hal-03011606

HAL Id: hal-03011606

<https://hal.science/hal-03011606>

Submitted on 21 Nov 2022

**HAL** is a multi-disciplinary open access archive for the deposit and dissemination of scientific research documents, whether they are published or not. The documents may come from teaching and research institutions in France or abroad, or from public or private research centers.

L'archive ouverte pluridisciplinaire **HAL**, est destinée au dépôt et à la diffusion de documents scientifiques de niveau recherche, publiés ou non, émanant des établissements d'enseignement et de recherche français ou étrangers, des laboratoires publics ou privés.



Distributed under a Creative Commons Attribution - NonCommercial 4.0 International License

# Effect of Thermal and Vibrational Combined Ageing on QFN Terminal Pads Solder Reliability

F. Arabi, A. Gracia, J-Y. Delétage, H. Frémont

Univ. Bordeaux, IMS, UMR 5218, F-33405 Talence, France

**Abstract** – Automotive environment generates vibration and temperature fluctuation, which reduces the life of electronic boards. The heavy trucks passing at relatively high speed on uneven road pavement is considered as the main reason of the traffic vibration. In fact, interaction between wheels and road surface causes a dynamic excitation which generates waves propagating in the soil affecting nearby structures. In addition, Thermal Cycling Test reveals the strict impact of environment conditions and slow cycles of temperature caused during operation. In this paper, vibration tests are performed continuously throughout thermal cycling to investigate the combined effect of temperature and vibration on the SAC305 solder of Quad Flat No-lead (QFN) terminals pads bonded on Printed Circuit Board (PCB). Power Spectral Density (PSD), which can be linked to the strain rate, is calculated from the acceleration, during combined ageing. Experimental results imply that the number of combined cycles affects the PCB responses: the value of the first natural frequencies and the corresponding PSDs. Fifty thermal cycles of combined thermal cycling and fatigue random vibration tests have been carried out on 100 QFN terminal pads solder. Statistical evaluation of the State of Health of the solder showed that cracking has started in 68% of them. An in-depth analysis was conducted to understand the reasons behind this degradation. On the other hand, an accurate numerical model for simultaneous combined thermal cycling and vibration simulation is developed and validated using experiments. These simulations make it possible to assess the displacement evolution due to combined loadings.

## 1 Introduction

Automotive environment generates vibration, which can be damaging for electronic boards and packages. They are exposed simultaneously to high temperature and dynamic loads when they are mounted on automotive systems. Both conditions, high temperature and vibrations, contribute to the failures in such systems. Single, sequential as well as simultaneous experiments introducing vibration, thermal and thermomechanical loads must be conducted to cover the effects of these conditions on the reliability of typical electronic packages. In fact, combined temperature and vibration is a type of testing that recreates environments that best approximate actual operating environments. Besides degradation effects as delamination, corrosion, thermo-migration and electromigration etc. solder fatigue is still a major failure mechanism leading to system fails. In fact, the solder joint has 3 functions: mechanical function which is the chip support, thermal function as the dissipation of the calories generated by the semiconductor and electrical function which is the passage of the electric current. As a major problem in recent years, solder fatigue was chosen as the degradation mechanism of interest. The present paper contains three sections. The first part presents an in-depth state of the art of the current knowledge about the reliability of electronic packages. In the second part, the thermal and vibrational combined ageing methodology is described. The effects of this combined aging on the solder reliability are analyzed and discussed. Finally, an accurate numerical model for simultaneous combined thermal cycling and vibration simulation is developed. The goal of these simulations is to assess the displacement and the strain rate evolution versus the number of combined cycles and to study the different interactions between phenomena which are due to combined loading. Experiments were conducted to validate simulation results.

## 2 Literature review

Much of the research in the area of solder joints reliability is based on thermal cycling which is considered as a low cycle fatigue test. Thermal and thermomechanical behavior of electronic packages has received extensive attention and has

been studied by many researchers [1] [2].

The damaging effect of single vibrational loads is also well documented [3]-[7]. Life prediction and aging theories under vibrations is well formalized. Liu *et al.* [8] performed random vibration and then correlated the Power Spectral Density (PSD) levels with the observed failure modes to assess the high cycle fatigue of SAC305 solder. Yu *et al.* [9] conducted sine sweep vibration test and Finite Element Analysis (FEA) to estimate the solder lifetime of SAC solder joints. They evaluated the fatigue life of a Ball Grid Array (BGA) assembly under random vibrations. Libot *et al.* [10] developed a new approach for SAC305 mechanical fatigue using simulation and experiments.

However, there is little data in the literature about combined aging, namely sequential and simultaneous. Effect of sequential combined ageing was presented in a previous work [11]. Experimental results implied that temperature significantly affects the PCB responses. Temperature variation leads to striking differences in dynamic response intensity. Karsten *et al.* [12] have worked on solder joints of ceramic capacitors which were stressed with single temperature shock and vibration loads. It was observed that the number of cycles to failure during temperature cycling with prior vibration is about two-thirds of the number of cycles to failure during temperature shock testing. Simultaneous aging remains the more realistic test as it best represents the field of use. However, it is difficult to study.

Lall *et al.* [13] performed simultaneous high temperature and vibration on SAC Electronics to assess its reliability. Results indicate that solder joint failures were predominantly observed at area-array components. Simulation model and experimental data indicated that the corner leads show the highest propensity for failure.

Hamasha *et al.* [14] studied aging of lead-free for harsh environment applications. It was observed that all solders, tested under combined higher temperature and higher vibration, are cracked.

Rögen *et al.* [15] have studied the effect of underfill on the propagation of cracks. It was observed that the addition of an underfill to the joint interface also seems to have inhibited

crack propagation otherwise encountered after exposure to temperature cycling and vibration.

Thermal cycling and vibration combined tests are usually studied using separate sequential tests. Then, the accumulation of the damages caused by both fatigues is done by Miner's cumulative damage model [16]. Scientifically, this model does not consider the different interactions between phenomena due to combined test. In fact, it is highly probable that it would have a relaxation of stress at vibration moments. Barker *et al.* [17] have studied combined vibrational and thermal solder joint fatigue by superposing the damage accumulated from both loads. They examined the solder life predictions by superposing the thermal and vibrational strains utilizing the generalized Coffin-Manson equation and Miner's rule. The result reveals that the life predictions have a high sensitivity to solder properties.

Since electronic packages undergo combined loading conditions in the field of use, a combined lifetime testing for development and qualification purposes is recommended. Lifetime models need to be developed covering the different loads for reproducing the field conditions. In this paper, the effects of combined test (Vibration & T-cycles) is studied. The quality of the solder State of Health (SoH) before, during and after aging is investigated. In the other hand, an accurate model of simultaneous combined test is developed using a continued perturbation of thermal loadings by mechanical ones.

### 3 Experiments

#### 3.1 Test equipment

In automotive environment, the heavy trucks passing at relatively high speed on uneven road pavement generate an important vertical vibration [18]. Therefore, a thermal chamber associated with a vertical vibration is used to study the packaging reliability (see Fig. 1). The thermal chamber is CLIMATS 90T-55/4 allowing Rapid Temperature Cycling (RTC). Vibration test is performed by an air-cooled shaker, LDS V555, whose characteristics are listed in Table 1. Furthermore, the sample needs an additional tool to be mounted on the shaker. The average weight of commonly used support tools is about 2kg. Therefore, it is very important to take into consideration the shaker limits because increasing weight decreases acceleration limits.



Fig. 1. Thermal chamber associated with a vertical vibration  
Table 1. LDS V555 air-cooled shaker characteristics

Shaker	Characteristics
Maximum sine force	939N

Maximum acceleration	100g ( $g = 9.81\text{m/s}^2$ )
Usable frequency range	5-6300Hz
Maximum weight	5kg (4Kg + head extender kit)

#### 3.2 Test profile

A combined test of thermal cycling and vibration is performed. The combined test profile, shown in Fig. 2, is chosen according to the automotive thermal cycling conditions STANDARD-ISO 16750 and random vibration [19]-[21]. This standard concerns electric and electronic systems/components for vehicles. It describes the potential environmental stresses and specifies tests and requirements recommended for the specific mounting location on/in the vehicle. The samples are exposed to a Rapid Temperature Cycling (RTC): from  $-40^\circ\text{C}$  to  $+125^\circ\text{C}$ , 60 minutes dwell time for low temperature level, 90 minutes dwell time for high temperature level,  $1^\circ\text{C}/\text{min}$  ramp rate when the temperature is below the ambient ( $20^\circ\text{C}$ ) and  $1.5^\circ\text{C}/\text{min}$  ramp rate when the temperature is above the ambient. The random vibration parameters: Root mean square acceleration and power spectral density (PSD) Vs. Frequency are listed in Table 2.

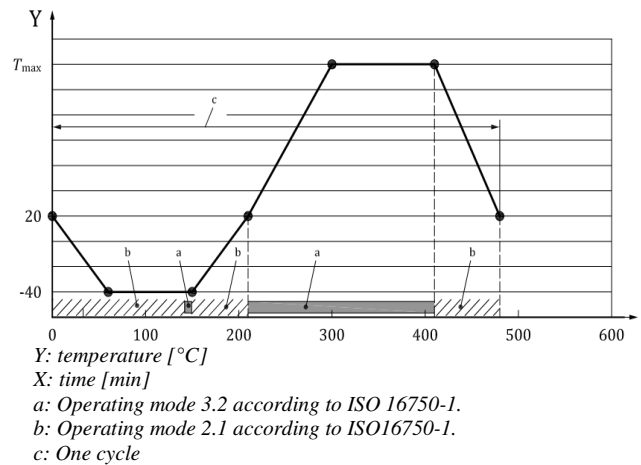


Fig. 2. Temperature profile for the vibration test.

Table 2. Random vibration parameters

Frequency [Hz]	PSD [ $(\text{m/s}^2)^2/\text{Hz}$ ]
100	5.02
2000	5.02
RMS acceleration: $97.7 \text{ m/s}^2 (9.96 \text{ g})$	

#### 3.3 Test vehicle

21 boards of  $155 \times 11 \times 1.6 \text{ mm}^3$  PCB are used in this study. The PCB contains 4 layers of copper, 2 layers of FR4-core and 3 layers of PREPREG with a total thickness of 1.6 mm. 25 packages are bonded on each board (see Fig. 3). The assemblies are not a prototype and they were made on a large production line. Its dimensions allow to make 5 components at the small side. To keep the symmetry basic, 5 components were bonded at the large side. This configuration allows studying the effect of QFN's (Quad Flat Pack No-Lead) emplacement. The packages are QFN40\_WF (Wettable Flanks)  $6 \times 6 \text{ mm}^2$ . The die dimensions are  $2 \times 1.5 \times 0.25 \text{ mm}^3$ .

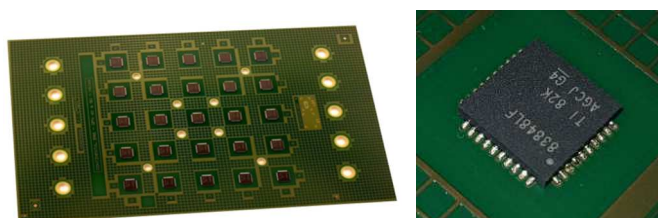


Fig. 3. Samples: PCB assembly with 25 soldered QFNs with WF terminal pads

### 3.4 Description of mounting and fixing

To increase the statistical significance of the results, three boards were tested simultaneously. To be sure to apply the same dynamic condition on each board, the length of the spacers was first varied using two boards in parallel (Fig. 4). Results presented in Table 3 showed that decreasing the distance of the stem between the two boards decreases the disparity of the PSD values. So, the value of  $d=12$  mm for the spacers was chosen. Results confirmed the same dynamic response whatever their position.

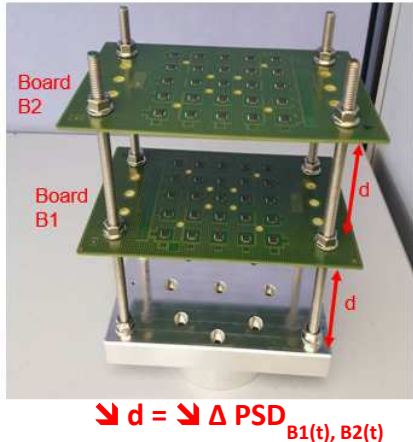


Fig. 4. Boards mounting and accelerometers fixing

Table 3. Dynamic response of parallel mounted boards Vs distance between boards

$d$ (mm)	$\Delta PSD$ [ $(m/s^2)^2/Hz$ ]
60	0.42
50	0.37
40	0.22
30	0.12
20	0.05
12	0.02

After choosing the minimal distance  $d=12$ mm as the distance between boards, a preliminary vibration test was conducted this time on 3 boards. They are mounted in parallel and vibrated simultaneously (see Fig. 5). This allows three readouts (RO) instead of one. The result showed the same dynamic response whatever their position. Acceleration is measured using a piezoelectric charge accelerometer designed for high-frequency low weight measurements. It's a B&K Type 4393 V sensor and it weighs 2.4 gram. For each board, an accelerometer is fixed beside the central QFN in a way that does not interfere with the results.

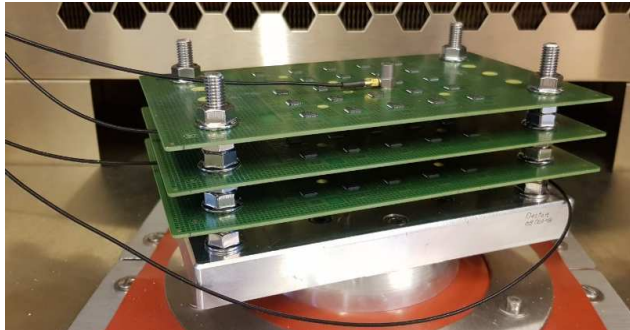


Fig. 5. Boards mounting and accelerometers fixing

### 3.5 QFN terminal pads

A QFN is a small size, lead-less plastic package with a low profile, moderate thermal dissipation, and good electrical performance. It is a surface mount package with metallized terminal pads located at the bottom surface of the package. QFN has terminal pads along the four edges of the bottom surface. QFN is designed with the die attach pad exposed at the bottom side to create an efficient heat path to the PCB. Heat transfer can be further facilitated by metal vias in the thermal land pattern of the PCB. The exposed pad also enables ground connection. There are two kinds of terminal pads: fully exposed terminal pads and Wettable Flanks terminal pads (WF). The latter promotes solder wetting for the formation of a solder fillet. The quality of the two terminal pads technologies allowed to determine which one will be investigated during ageing.

Cross-section inspection of QFN with fully exposed terminal pads showed that all of them present a delamination of the solder meniscus as visible in Fig. 6. In fact, fully exposed terminal pads shape presents a 90-degree angle, which is not favorable to a good adhesion; so this defect probably occurred during the assembly process.

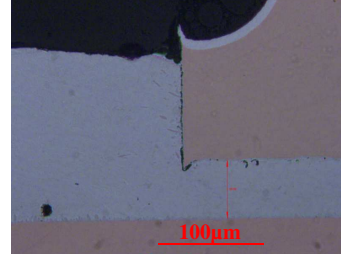


Fig. 6. Separation between the meniscus and the terminal pad edge of QFN with fully exposed terminal pads

In the other hand, the Wettable Flanks terminal pads present a big ratio of voids as shown in Fig. 7. These voids may have a negative effect on the solder SoH, but this kind of terminal pads eliminates the problem of delamination observed on fully exposed terminal pads. In addition, these uniform solder fillets enable inspection of solder failures using automatic optical inspection (AOI) and avoid the need for x-ray inspection, with additional cost and layout restrictions for the PCB. For these reasons, the QFN with Wettable Flanks terminal pads were chosen for this study.

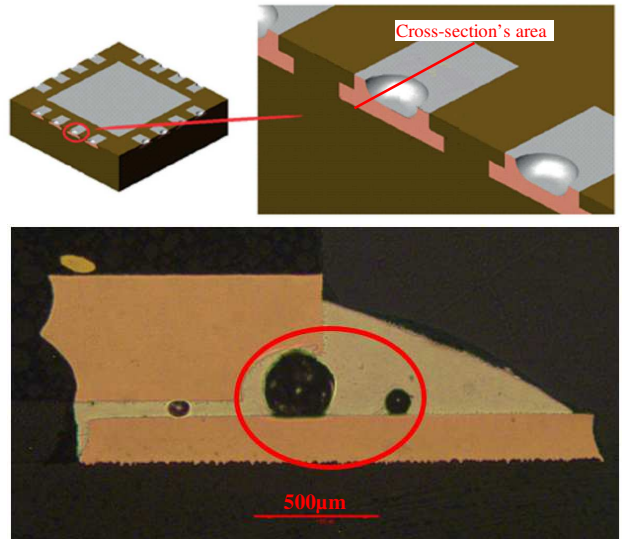


Fig. 7. Cross-section images of the meniscus of a QFN40 with Wettable Flanks terminal pads

### 3.6 Ageing results

Four boards are submitted to either 5, 10, 15 or 50 cycles of combined ageing. The PSD as a function of frequency was measured on these 4 boards (see Fig. 8). An evolution of the dynamic responses upon the first 15 combined cycles is visible. However, the dynamic response after 50 cycles is almost identical to that obtained after 10 cycles. Before 15 cycles, the first natural frequency and the corresponding PSD increased as the ageing continues.

Two hypotheses can be put forward to explain this behaviour:

The frequency evolution during ageing could be due to a sample mass variation and/or its physical properties variation. A lower mass and/or a stiffer material increase the natural frequency; a higher mass and/or a softer material lower the natural frequency [22]. As the air temperature increases during ageing, vapor pressure increases. This could speed up outgassing and evaporation, both of which reduce the mass of the impure metal. Knowing also that temperature influences the material stiffness and therefore the natural frequencies. The PSD evolution during ageing could be due to the stress accumulation. Ali *et al.* proved that the PSD value depends on strain [23]. Therefore, the PSD increases because the sample accumulates stresses when the number of cycles increases.

Boards are cross-sectioned to study the evolution of the solder State of Health (SoH). Optical microscopy inspection of terminal pad attachments did not reveal any changes during the first 15 cycles. However, after 50 cycles, 68% of the terminal pad solder were cracked. Fig. 9 shows the cracks' propagation throughout the solder. The solder SoH could explain why the value of the natural frequency measured at 50 cycles did not follow the same pace as that measured during the first readouts 5, 10 and 15 cycles. In fact, the stress level at 50 cycles was enough to initiate the crack. Then the crack propagated to attenuate the stress.

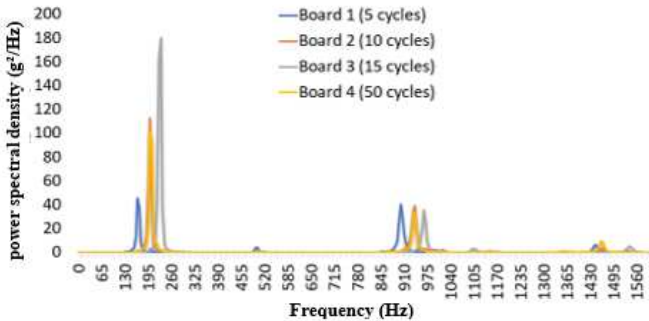


Fig. 8. Evolution of the dynamic responses during combined ageing -50 cycles

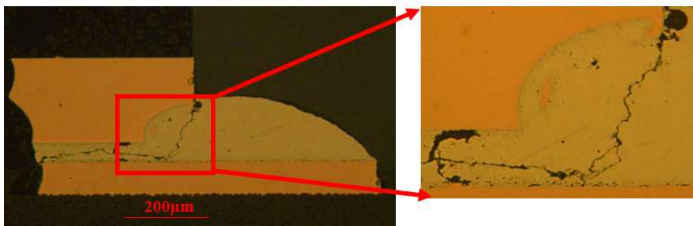


Fig. 9. Image of optical inspection after 50 cycles – QFN terminal pads solder

## 4 Finite Element Simulations

### 4.1 Context

Since it was assumed that vibration might affect QFN terminal pads' stresses and strains, we developed an accurate model representing the strain-stress due to dynamic combined

loading. In [11] we developed such a model on PCBs without component to study the effect of sequential combined loadings. It was validated by correlating the relationship between experimental and modelling results. In this section, a simulation model is presented to study the effect of simultaneous combined vibrational and thermal loads on PCB populated with QFNs. It was developed in two phases. The first simple model considers only one QFN, the second one takes all the QFNs into account. The model aims at quantifying the stress and the strain at the terminal pads and at determining the more constrained terminal pads. Experimental boards are modelled using ANSYS®.

### 4.2 Material properties

#### 4.2.1 PCB

FR4 is considered as an orthotropic material, contrary to copper which is considered as isotropic. This complex PCB needs to be characterized at different temperatures, to extract user input parameter temperature dependent for combined simulations. This is mandatory to take into consideration the interactions between mechanical and thermal loadings. Thermo-mechanical and mechanical properties of FR4 are considered as a function of the temperature and following the three directions. These properties are Young's modulus, Poisson's ratio, shear modulus, coefficient of thermal expansion, specific heat and density. These properties were taken from [11] and recalled in Table 4.

#### 4.2.2 QFN

When the QFN is completely modelled, the materials of terminal pads, thermal pad, component and mold compound are considered. The properties of these materials are listed in Table 4.

#### 4.2.3 Solder joints

Solder joints are commonly modeled as a viscoplastic material. Anand model has been considered for SAC305 solder. Anand parameters used in the FE model were extracted from [24] and listed in Table 5.

Table 4. Material properties

Material	E (GPa)	G (GPa)	v	D (g.cm⁻³)
FR4	22(x)	3.5(xy)	0.11(xy)	1.85
	22(y)	2.5(xz)	0.28(xz)	
	9.8(z)	2.5(yz)	0.28(yz)	
SAC305	50	-	0.45	7.37
Copper	124	-	0.33	8.96
Silicone	163	-	0.35	2.33
Epoxy	18.9	-	0.3	2.25
QFN simple block	50.83	-	0.33	2.78

Table 5. Anand parameters used in the FE model

Parameter	Units	Value
$s_0$	MPa	21
$Q$	K⁻¹	9320
$R$	-	
$A$	-	3501
$\xi$	-	4
$m$	-	0.25
$h_0$	MPa	18
$\hat{s}$	MPa	30.2
$n$	-	0.01
$a$	-	1.78

### 4.3 Modelling

To better mimic the real configurations, all QFNs are modelled. The central QFN is modelled with its terminal pads, thermal pad and different solder attaches. However, the other 24 QFNs are designed as simple blocks in order to study their effect on the shrinkage of the structure during cooling and warming. This configuration makes it possible to take in consideration the mechanical effect of the QFNs without having too much elements (see Fig. 10). The best choice is to simulate the real package and to consider a new material whose parameters are averaged over the elements' volumes. For that purpose, the mechanical properties of this multilayer are determined using simulations.

To calculate volume average of variable parameters, the formula given in Eq.1 is used.

$$P = \sum_{i=0}^n \frac{P_i * V_i}{V} \quad \text{Eq.1}$$

Where  $P_i$  is the parameter of the element  $i$ ,  $V_i$  is the volume of the element,  $V$  the sum of the volumes of all elements of different materials which equals the volume of the simple block and  $P$  is the parameter of the simple block. The parameters of the simple mechanical block are calculated and added to Table 4.

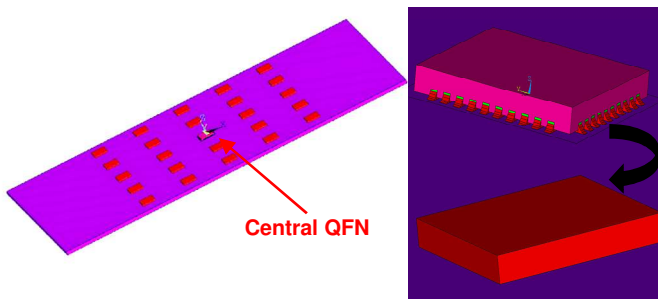


Fig. 10. PCB assembly with 25 QFNs and Transition from QFN model to simple block model

### 4.4 Simulation results

5 combined cycles (Vibration ( $5.02 \text{ m/s}^2/\text{Hz}$ ) and T-cycles [ $-40^\circ\text{C}/125^\circ\text{C}$ ]) were simulated on a PCB assembly with 25 QFNs: one central QFNs and 24 simple blocks representing other QFNs. Results show that the calculated power spectral density is almost identical to that measured as shown in Fig. 11.

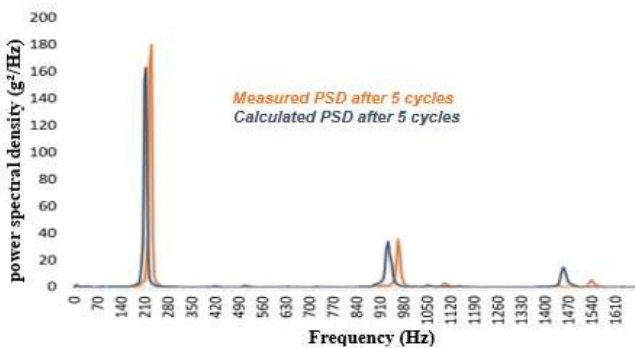


Fig. 11. Calculated PSD response Vs. Frequency

The distribution of simulated equivalent stresses for the terminal pads, terminal solder pads and thermal solder pads at the first frequency is presented in Fig. 12. It shows that the

terminal solder pads are the most constrained and especially those which are normal to the length of the PCB as they undergo the most significant bending. A very important level of stress (ave. eq. stresses of  $\sim 200\text{MPa}$  and peak stress of up to  $300\text{MPa}$ ) was observed on some solder meniscus (where the red colour is located). It is especially the pads of the QFN corners which undergo the maximum stress due to their position. These important values could depend a little bit on the physical properties of the materials as well as the applied FE Anand model for SAC material. However, that does not prevent from saying that it reflects a little the reality and the stress undergone by these pads located at the QFN corners [25]. Several other reasons can be behind this level of constraints. A corner is an irregularity in the geometry or material of a structural component that cause an interruption to the flow of stress and therefore generates stress concentrations. The quantity of material to support by the pads solders' located on the corners is more important than that supported by two linear pads considering the distance between them. These results obtained after only 5 cycles could give a line of explanation of the experimental result. In fact, the solder of terminal pads cracking observed in experimentation could be due to the CTE mismatch of the materials as well as the mechanical stresses caused by higher level package integration and module assemblies as showed in simulations.

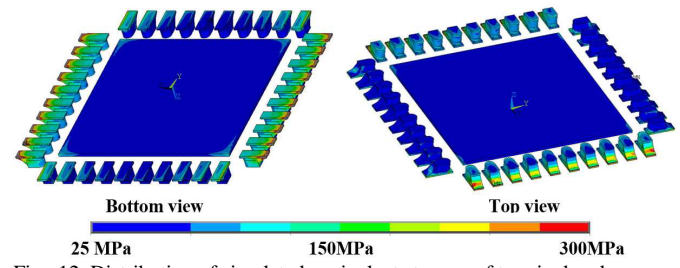


Fig. 12. Distribution of simulated equivalent stresses of terminal pads, terminal and thermal pads solders', from FEM simulation at the first frequency

### 5 Conclusion

The present work has examined the effect of simultaneous combined ageing (vibration and T-cycles [ $-40/125^\circ\text{C}$ ]) on the dynamic response of a PCB populated with QFNs using simulations and experiments. These assemblies are not prototypes and they were made on a large production line.

Vibration tests are performed continuously throughout thermal cycling to investigate the combined effect of temperature and vibration on the SAC305 solder of Quad Flat No-lead (QFN) terminals pads bonded on Printed Circuit Board (PCB). Experimental results imply that the number of combined cycles affects the PCB responses: the value of the first natural frequencies and the corresponding PSDs. 50 cycles of combined temperature cycling and fatigue random vibration test has been carried out on 100 QFN terminal pads solder. Statistical evaluation of the SoH of these terminal pads solder showed that cracking has started in 68 of them. An in-depth analysis was conducted to understand the reasons behind this degradation. The observed Freq Vs. PSD variations have been understood thanks to the comparison of the solder SoH. According to the ageing outcomes and the microscopy images, the stress level occurred at 50 cycles was enough to initiate the cracks at the voids' outlines. Then the crack propagates between two voids so as to attenuate the stress as the vibrations accelerate the crack propagation.

The presented methodology of simultaneous combined

simulation represents a significant opportunity to reduce the cost and time needed for experimental testing even under combined testing environment. FE simulations have shown a good accuracy using the software with the interfering function to combine the instantaneous thermal and mechanical loads at each node. This was required to perform a reliable test set-up in order to compare the simulation and the experimental results, to assist the drifts and correct them. In this work, the opportunity to quantify the displacement and the stress under combined testing is demonstrated. These simulations allow quantifying the accumulation of stresses versus the first cycles. Good agreement was obtained between simulation and experimental results. The samples will be subjected to further cycles in order to confirm this correlation. It could give an approximate indication about the number of cycles undergone by the solder joints before failure. If the correlation is not significant, the developed multiphysics model could be corrected using experimental results to reduce the drift between simulations and experience. Further evaluation of the influence of dwell time and ramp rates will be investigated both experimentally and from numerical simulations.

### Acknowledgment

The authors gratefully acknowledge the support and the financial provided by the Federal Ministry of Education and Research (FMR) under grant number 16ES0488K-16ES0502, 16ES0737 for the research project TRACE “Technology ReAdiness process for Consumer Electronics” that forms the basis for the present work.

### References

- [1] Berthou, M., Retailleau, P., Frémont, H., Guédon-Gracia, A. and Jéphos-Davennel, C., 2009. Microstructure evolution observation for SAC solder joint: Comparison between thermal cycling and thermal storage. *Microelectronics Reliability*, 49(9-11), pp.1267-1272.
- [2] Vandevelde, B., Gonzalez, M., Limaye, P., Ratchev, P., & Beyne, E. (2007). Thermal cycling reliability of SnAgCu and SnPb solder joints: a comparison for several IC-packages. *Microelectronics Reliability*, 47(2), 259-265.
- [3] Nicholas, T. High cycle fatigue: a mechanics of materials perspective. Elsevier, 2006.
- [4] Schriener, T., Maximilian H., and Martin M. "Vibrational resistance investigation of an IGBT gate driver utilizing Frequency Response Analysis (FRA) and Highly Accelerated Life Test (HALT)." In CIPS 2018; 10th International Conference on Integrated Power Electronics Systems, pp. 1-6. VDE, 2018.
- [5] Zhou, Y., Scanff, E., Dasgupta, A., "Vibration Durability Comparison of Sn<sub>37</sub>Pb vs SnAgCu Solders," Proc. of IMECE2006, Chicago, Illinois, November 2006.
- [6] Berthou, M., Lu, H., Retailleau, P., Frémont, H., Guédon-Gracia, A., Davennel, C. and Bailey, C., 2010, August. Vibration test durability on large BGA assemblies: Evaluation of reinforcement techniques. In 2010 IEEE CPMT Symposium Japan (pp. 1-4). IEEE.
- [7] Arabi, F., A. Gracia, J-Y. Delétage, and H. Frémont. "Vibration test and simulation of printed circuit board." In Thermal, Mechanical and Multi-Physics Simulation and Experiments in Microelectronics and Microsystems (EuroSimE), 2018 19th International Conference on, pp. 1-7. IEEE, 2018.
- [8] Liu, F., & Meng, G. (2014). Random vibration reliability of BGA lead-free solder joint. *Microelectronics Reliability*, 54(1), 226-232.
- [9] Yu, D., Al-Yafawi, A., Nguyen, T. T., Park, S., & Chung, S. (2011). High-cycle fatigue life prediction for Pb-free BGA under random vibration loading. *Microelectronics Reliability*, 51(3), 649-656.
- [10] Libot, J. B., Arnaud, L., Dalverny, O., Alexis, J., Milesi, P., & Dulondel, F. (2016, April). Mechanical fatigue assessment of SAC305 solder joints under harmonic vibrations. In 2016 International Conference on Electronics Packaging (ICEP) (pp. 231-236). IEEE.
- [11] Arabi, F., A. Gracia, J-Y. Delétage, and H. Frémont. "Sequential combined thermal cycling and vibration test and simulation of printed circuit board." *Microelectronics Reliability* 88 (2018): 768-773.
- [12] Meier, K., Mike, R., Andreas, S., and Wolter, K-J. "Reliability study on chip capacitor solder joints under thermo-mechanical and vibration loading." In 2014 15th International Conference on Thermal, Mechanical and Multiphysics Simulation and Experiments in Microelectronics and Microsystems (EuroSimE), pp. 1-7. IEEE, 2014.
- [13] Lall, P., Limaye, G., Suhling, J., Murtaza, M., Palmer, B., & Cooper, W. (2012, May). Reliability of lead-free SAC electronics under simultaneous exposure to high temperature and vibration. In 13th InterSociety Conference on Thermal and Thermomechanical Phenomena in Electronic Systems (pp. 753-761). IEEE.
- [14] Evans, J. L., Bozack, M., & Johnson, W. (2018, February). Long-term isothermally aged concerns for SAC lead-free solder in harsh environment applications. In 2018 Pan Pacific Microelectronics Symposium (Pan Pacific) (pp. 1-7). IEEE.
- [15] Rörgren, R., Tegehall, P. E., & Carlsson, P. (1998). Reliability of BGA packages in an automotive environment. *Journal of Surface Mount Technology*, 11, 35-44.
- [16] Qi, H., Michael O., and Michael P. "Modeling of combined temperature cycling and vibration loading on PBGA solder joints using an incremental damage superposition approach." *IEEE Transactions on Advanced Packaging* 31.3 (2008): 463-472.
- [17] Barker, D., J. Vodzak, A. Dasgupta, and M. Pecht. "Combined vibrational and thermal solder joint fatigue—A generalized strain versus life approach." *Journal of Electronic Packaging* 112, no. 2 (1990): 129-134.
- [18] Beer, M.D., 1996. Measurement of tyre/pavement interface stresses under moving wheel loads. *International Journal of Heavy Vehicle Systems*, 3(1-4), pp.97-115.
- [19] ISO FDIS 16750-1:2006: Road Vehicles - Environmental conditions and testing for electrical and electronic equipment - Part 1: General, Geneva, Switzerland: International Organization for Standardization
- [20] ISO FDIS 16750-3:2006: Road vehicles - Environmental conditions and testing for electrical and electronic equipment - Part 3: Mechanical loads, Geneva, Switzerland: International Organization for Standardization
- [21] ISO FDIS 16750-4:2006: Road vehicles - Environmental conditions and testing for electrical and electronic equipment - Part 4: Climatic loads, Geneva, Switzerland: International Organization for Standardization
- [22] Myklestad, N.O., 2018. Fundamentals of vibration analysis. Courier Dover Publications.
- [23] Ali, M. B., et al. "Correlation of absorbed impact with calculated strain energy using an instrumented Charpy impact test." (2013).
- [24] Lövberg, A., Tegehall, P-E., Wetter, G., Brinkfeldt, K., and Andersson, D. "Simulations of the impact of single-grained lead-free solder joints on the reliability of ball Grid Array components." In 2017 18th International Conference on Thermal,

Mechanical and Multi-Physics Simulation and Experiments in Microelectronics and Microsystems (EuroSimE), pp. 1-10. IEEE, 2017.

- [25] Krishnamurthy, S., Deshpande, A., Islam, M.M. and Agonafer, D., 2016, May. Multi design variable optimization of QFN package on thick boards for enhanced board level reliability. In 2016 15th IEEE Intersociety Conference on Thermal and Thermomechanical Phenomena in Electronic Systems (ITherm) (pp. 1546-1550). IEEE.